



Cite this: *Mater. Adv.*, 2024, 5, 7377

## Low cost paints reinforced with an $\text{Al}_2\text{O}_3/\text{Y}_2\text{O}_3$ /graphene nanocomposite for fire-resistant wood coating applications

Ahmed El-Tantawy,<sup>a</sup> Ibrahim M. Hassan,<sup>a</sup> Omayma A. El-kady,<sup>b</sup> Ahmed. I. Ali,<sup>cd</sup> Jong Yeog Son<sup>cd</sup> and Nasser. M. Ayoub<sup>a</sup>

Low-cost eco-friendly 10wt% $\text{Al}_2\text{O}_3$ /5wt% $\text{Y}_2\text{O}_3$ /graphene (graphene nanosheets (GNSs): 0.5, 1.0, 1.5, 2.0, 2.5wt%) nanocomposite powders were fabricated using a powder metallurgy technique. X-ray diffraction and FE-SEM confirmed that the phase and morphology of the surface are homogenous and crack-free with nanoscale particles. Thermal analysis (TGA/DSC) confirmed the decomposition sequence as a function of temperature. Furthermore, X-ray photoelectron spectroscopy (XPS) was investigated in a comparison between samples of two compositions of oxygen, aluminum, and yttrium atoms at 75 eV, 158 eV and 158 eV at the equivalent of 1200 cps, 4200 cps, and 4600 cps, respectively. The results for fire resistance confirmed the impact of GNS percentage on fire resistance and fire endurance, and in a rising temperature test. In addition, compared with the period in previous experiments (35 s), the sample with paint with 10wt% $\text{Al}_2\text{O}_3$ /5wt% $\text{Y}_2\text{O}_3$ /2.5wt%GNSs (2.5 g of graphene) had a fire resistance time of 887 s at  $T = 190$  °C. Thus, the present work demonstrated that low-cost and easily fabricated  $\text{Al}_2\text{O}_3/\text{Y}_2\text{O}_3/\text{GNSs}$  nanocomposite powders enhanced the properties of the wood-paint to be a good candidate in fire resistance applications.

Received 30th May 2024,  
Accepted 14th August 2024

DOI: 10.1039/d4ma00552j

[rsc.li/materials-advances](http://rsc.li/materials-advances)

## 1. Introduction

One of the most important types of crisis and disaster worldwide is fire, especially in homes with wooden foundations. The rapid spread of fire leads to disasters and a great loss of people and wealth in wood. Fire accidents spread worldwide and cause a great amount of global destruction, whether material or mental. Surface coating is a process undertaken to protect structural materials from harsh environmental problems such as corrosion,<sup>1</sup> mechanical abrasion,<sup>2</sup> and biofouling, and amelioration of fire hazards involves a multibillion-dollar market applied in residential, industrial<sup>3</sup> and defense industries. The total costs every year associated with these everlasting problems caused by lack of effective materials are enormous.<sup>4</sup> Fire incidents in transport, mainly involving private vehicles on public roads,

but also other types of transport including trains, aircraft and ships of numerous kinds, can have disturbing effects, resulting in mass loss of life and the destruction of buildings, infrastructure and personal property. It is also important not to underestimate the behavior of fire and its different characteristics. Typical fire development occurs over four consecutive stages: incipient, growth, fully developed and decay, with each stage having varying degrees of risk as the fire develops to the point of flashover and steady burning, where the involvement of firefighters becomes critical.<sup>5</sup>

Fire resistance is a critical feature; it includes the ability of a material or structure to resist fire or to slow down its rate. Fire safety is a serious matter everywhere and alarm is increasing in all nations because of the growth in the number of people and due to house construction materials. There are new cities consisting of some big buildings that are made using a diversity of inflammable materials causing alarm about fire safety. Lack of fire resistance is becoming a particular risk to life and protection of property. Although around the world there are several countries where buildings may be found that are not constructed according to a known standard of building codes.<sup>6</sup>

Based on the above scenario, due to the responsibilities of fire precautions, health and safety has become one of the subjects of study for researchers, with some groups searching for fire resistance and others searching for improvements in

<sup>a</sup>Department of Production Technology, Faculty of Technology and Education, Helwan University, Saray-El Qouqa, El Sawah Street, 11281 Cairo, Egypt

<sup>b</sup>Powder Technology Department, Central Metallurgical Research and Development Institute (CMRDI), P.O. Box 87, Helwan, Cairo, Egypt

<sup>c</sup>Basic Science Department, Faculty of Technology and Education, Helwan University, Saray-El Qouqa, El Sawah Street, 11281 Cairo, Egypt.

E-mail: Ahmed\_Ali\_2010@techedu.helwan.edu.eg

<sup>d</sup>Department of Applied Physics and Institute of Natural Sciences, College of Applied Science, Kyung Hee University, Suwon 446-701, Republic of Korea.  
E-mail: jyson@khu.ac.kr



materials against fire such as coatings, whilst different groups are working on the computation of ways to protect humans from accidental fires.<sup>7</sup> Researchers have developed several compositions to enhance fire resistance in materials and structures. They have designed compositions with thermal stability at high temperature to avoid the quick spread of fires.<sup>8</sup> Some common compositions include fire-resistant coatings, containing fire-retardant chemicals that afford a shielding sheet, avoiding explosion and the spread of fire.<sup>9,10</sup> Intumescent coatings expand when subjected to warmth, founding an insulating layer that shields the original material. Moreover, there are excellent fire-resistant materials with insulation properties, such as cement-based mixtures, mineral wool, fiberglass, or foam, and specific glass compositions can be used to enhance fire resistance by reducing heat transfer.<sup>11</sup> Compositions for fire resistance play a vital role in minimizing damage and ensuring the safety of individuals. Wood coating still needs more research to find candidate materials for application to fire safety. By incorporating effective compositions and materials, structures can withstand high temperatures and slow down the spread of flames. Factors such as temperature tolerance, ignition resistance, structural integrity, and smoke emissions play a crucial role in determining the overall fire resistance of a material or structure. By prioritizing fire resistance, we can mitigate risk and create safer environments for all.<sup>12,13</sup>

Fire resistance in applications of composites to wood is of extreme importance to ensure safety and protect valuable structures. By incorporating fire-retardant additives, utilizing surface treatments, or exploring alternative composite materials, the fire resistance properties of wood composites can be significantly enhanced. However, challenges related to durability, cost-effectiveness, and environmental impact must be addressed to pave the way for future advances in this field.<sup>14</sup> The development of highly fire-resistant wood composites is within reach, providing a promising solution for a wide range of applications.<sup>15,16</sup> The coating process is defined as the application of a layer of material that covers the surface of a bulk material to achieve specific properties. The search for materials that can resist fires, such as paint for wood or coatings using different composites is in the spotlight.<sup>10,17</sup>

Surface and bulk material protection is the major goal of functional coatings in the fight against corrosion, fouling, mechanical wear, microorganisms, and environmental damage, and for fire resistance.<sup>6</sup> Similarly, coating materials are extensively used in military applications, marine industries, medical instruments, electronic devices, and everyday household appliances.<sup>18</sup> A new generation of materials with high thermal stability has been developed to add to paints for protection against the spread of fire.<sup>19,20</sup> Substrates, such as wood and various metals, have been coated to make them more fire-retardant.<sup>21</sup>

Nanomaterials have revolutionized the field of fire resistance by offering unique solutions to combat fire hazards. With their exceptional properties and structures, nanomaterials like carbon nanotubes, graphene oxide, metal oxide nanoparticles, nano-clay, and nano-aluminum have significantly enhanced the fire resistance of various materials. The incorporation of

these nanomaterials into polymers, coatings, and composites has shown promising results in mitigating the risks associated with fire.<sup>22,23</sup> Thus the goal of the present work is focused on a fire-retardant coating and finding nanocomposites to apply to many organic and inorganic substrates for fire protection by reducing the spread of flames and reducing heat transmission.<sup>9</sup>  $\text{Y}_2\text{O}_3$ ,  $\text{Al}_2\text{O}_3$ , and graphene nanocomposites have been proposed to show exciting opportunities for increasing highly effective fire-resistant materials. The combination of both  $\text{Y}_2\text{O}_3$  and  $\text{Al}_2\text{O}_3$  gives the paint thermal stability as well as graphene's electrical conductivity and mechanical strength creating a powerful defense against fire. With this research, these composites hold significant potential to revolutionize fire safety across various industries, ultimately saving lives and overcoming the overwhelming influence of fires.

In this article, we fabricated nanocomposites of  $\text{Al}_2\text{O}_3/\text{Y}_2\text{O}_3$ /graphene with a different ratios of graphene for fire resistance using a powder metallurgy technique. Characterizations including XRD, SEM, TGA/DSC and XPS were done on the samples. Experiments to check the fire speed rate were investigated. Our experimental data for painting composites can be used as an indication of fire safety for wood fire-resistant applications.

## 2. Experimental methods

### 2.1. Materials and composites

**2.1.1. Powder preparation.** Graphene nanocomposites were fabricated using a powder metallurgy technique. Graphene nanosheet powder with a particle size of 3–10  $\mu\text{m}$  and a purity of 99.6%, yttrium oxide ( $\text{Y}_2\text{O}_3$ ) powder with a particle size of 4–5  $\mu\text{m}$  and a purity of 99.7, and aluminum oxide ( $\text{Al}_2\text{O}_3$ ) powder with a particle size of 3  $\mu\text{m}$  were used for the preparation of five nanocomposites,<sup>24–26</sup> graphene nanosheets (0.5, 1.0, 1.5, 2.0, and 2.5wt%) were added to samples of 5wt% $\text{Y}_2\text{O}_3$ /10wt% $\text{Al}_2\text{O}_3$ . The samples with different ratios of GNS nanocomposites were prepared by a mechanical alloying technique with a 10:1 ball to powder ratio at 100 rpm for 24 h of milling time; to avoid any oxidation, 2wt% ethanol and argon gas were used during the milling process. 20wt% of each composition was added to paints which were used to coat a wood substrate. The phase and microstructure of 10wt% $\text{Al}_2\text{O}_3$ /5wt% $\text{Y}_2\text{O}_3$ /GNSs powders and the consolidated composites were investigated by both X-ray diffraction and scanning electron microscopy.<sup>16</sup> Thermal analysis (TGA/DSC) was recorded with temperature rising from room temperature up to 550 °C for all the consolidated composites. X-ray photoelectron spectroscopy (XPS) was used to study the two prepared powder mixtures of 10wt% $\text{Al}_2\text{O}_3$ /5wt% $\text{Y}_2\text{O}_3$ /0.5wt%GNSs and 10wt% $\text{Al}_2\text{O}_3$ /5wt% $\text{Y}_2\text{O}_3$ /2.5wt%GNSs.

**2.1.2. Wood samples.** Plywood is a composite material manufactured from thin layers and it is an engineered wood from the family of manufactured boards, which also include medium-density fiberboard (MDF), oriented strand board (OSB), and particle board (or chipboard).<sup>13</sup> Plywood of a density of around 150–250 kg  $\text{m}^{-3}$ , purchased from a wood factory



Table 1 Nanocomposite powders used as reinforcement material for paints

Sample	Al <sub>2</sub> O <sub>3</sub>	Y <sub>2</sub> O <sub>3</sub>	Graphene	Paint	Total
1	0	0	0	100	100
2	10	0	0	90	100
3	10	5	0	85	100
4	10	5	2.5	82.5	100
5	10	5	5	80	100
6	10	5	7.5	77.5	100
7	10	5	10	75	100
8	10	5	12.5	72.5	100

(Ismailia City, Cairo) was prepared with dimensions of  $100 \times 100 \times 6$  mm<sup>3</sup> and dried in an oven at 100 °C for 24 h.<sup>14</sup>

**2.1.3 Wood paint.** The basic components of the paint consist of calcium carbonate, calcined clays, titanium dioxide, resins, ketones, dryers, stabilizers, silicones, oligomers, and sodium benzoate.<sup>15</sup> This composite was prepared by a mechanical milling technique at 100 rpm, with a 10:1 ball to powder ratio for 24 h. Then 20% of this composite powder (10wt%Al<sub>2</sub>O<sub>3</sub>/5wt%Y<sub>2</sub>O<sub>3</sub>/0.5wt% GNSs) was added to the paints on a wood substrate of  $100 \times 100 \times 6$  mm<sup>3</sup> dimensions with  $3 \pm 0.2$  paint thickness.

## 2.2. Characterization

**2.2.1. X-ray diffraction for powders.** The drying model used for the wood simple with dimensions  $220 \times 220 \times 1.5$  mm was 168 hours at room temperature. The paints reinforced with the prepared composite powders were used to treat the wood species by heat radiation of  $25$  kW m<sup>-2</sup> in the horizontal orientation during the test. SEM-XPS-XRD tests were used as follows.<sup>26</sup>

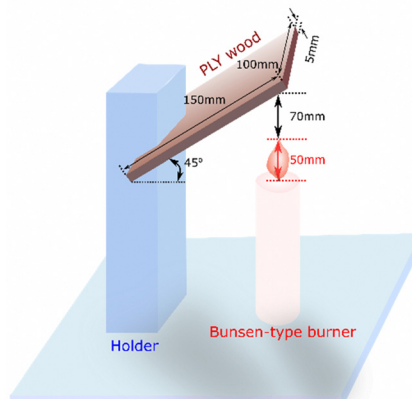
The microstructures (SEM) were investigated for a powder mixtures consisting of pure Al<sub>2</sub>O<sub>3</sub> nanoparticles, 10wt%Al<sub>2</sub>O<sub>3</sub>/5wt%Y<sub>2</sub>O<sub>3</sub>, and 10wt%Al<sub>2</sub>O<sub>3</sub>/5wt%Y<sub>2</sub>O<sub>3</sub>/xwt%GNSs ( $x$ : 0.5, 1, 1.5, 2, 2.5) on sample-coated wood with dimensions of  $1 \times 1$  cm<sup>2</sup>. The quantities of paint mixed with the nano mixture were as shown in Table 1.

## 2.3. Experimental measurement technique

Different proportions of graphene nanosheet by weight percentage of graphene (0.5, 1, 1.5, 2, 2.5) were mixed with 5wt% yttrium oxide and 10wt% aluminum oxide. The samples were dried at room temperature for 7 days before starting all the investigations. A flat cylinder with a thickness of 5 mm, 50 mm diameter was installed on the base to accommodate a fire candle, through which the fire was ignited on the sample, as shown in Fig. 1,<sup>17</sup> which shows a firing system for wood without paint, wood with paint free from any additives, and wood coated with paints with the prepared composite powders.

## 2.4. Coating preparation

The prepared nanocomposite powders used as a reinforcement material for the paints are shown in Table 1. The paint reinforced with the manufactured nanocomposites was coated on the surface of the wood substrate and dried at room temperature for at least 168 h, where the thickness of the fire-resistant coatings was  $3 \pm 0.2$  mm.<sup>19</sup>

Fig. 1 Fire resistance test system according to Iranian patent no. 67232.<sup>18</sup>

## 2.5. Fire resistance test

A fire resistance experiment was used to evaluate the performance of the paints reinforced with Al<sub>2</sub>O<sub>3</sub>/Y<sub>2</sub>O<sub>3</sub>/graphene nanocomposites. The experimental device is shown in Fig. 1. The base of the model had dimensions of  $220 \times 220$  mm<sup>2</sup>, and the model holder was installed on the base. A circular piece was installed on the base to hold the fire candle.<sup>20</sup> This experiment was repeated many times to ensure the reproducibility of the results.

## 3. Results and discussion

### 3.1. Microstructure of the fabricated paints

The developed composite powders dispersed in the paints at 20wt% were characterized with a scanning electron microscope (SEM) to analyze the homogenization and bonding between the constituents. This test depends on an electron beam to scan and magnify the images. SEM micrographs were obtained of samples containing: (a) pure Al<sub>2</sub>O<sub>3</sub>, (b) 10wt%Al<sub>2</sub>O<sub>3</sub>/5wt%Y<sub>2</sub>O<sub>3</sub>, (c) 10wt%Al<sub>2</sub>O<sub>3</sub>/5wt%Y<sub>2</sub>O<sub>3</sub>/0.5wt%GNSs, (d) 10wt%Al<sub>2</sub>O<sub>3</sub>/5wt%Y<sub>2</sub>O<sub>3</sub>/1wt%GNSs, (e) 10wt%Al<sub>2</sub>O<sub>3</sub>/5wt%Y<sub>2</sub>O<sub>3</sub>/1.5wt%GNSs, (f) 10wt%Al<sub>2</sub>O<sub>3</sub>/5wt%Y<sub>2</sub>O<sub>3</sub>/2wt%GNSs, and (g) 10wt%Al<sub>2</sub>O<sub>3</sub>/5wt%Y<sub>2</sub>O<sub>3</sub>/2.5wt%GNSs. The microstructure of the paint samples was reinforced with 10wt%Al<sub>2</sub>O<sub>3</sub>/5wt%Y<sub>2</sub>O<sub>3</sub>/xwt%GNSs ( $x$ : 0.5, 1.0, 1.5, 2.0, 2.5). All the samples show good homogeneity for all the constituents. As the percentage of graphene increases, some agglomeration takes place due to the high surface area of the graphene nanosheets.<sup>21</sup> The process during the fire, and the results showed a random distribution of graphene nanosheets on the samples, as seen from SEM. XRD results showed only the peaks corresponding to Al<sub>2</sub>O<sub>3</sub> and Y<sub>2</sub>O<sub>3</sub>, while graphene could not be detected due to its very low ratio. Yttrium and aluminum oxides were distributed homogeneously in the samples, and the results showed that aluminum oxide and yttrium oxide are very closely integrated inside the paints. In addition, no deposits were detected on the samples, and the tests were done using a model with a metal base with a metal holder installed in the end.



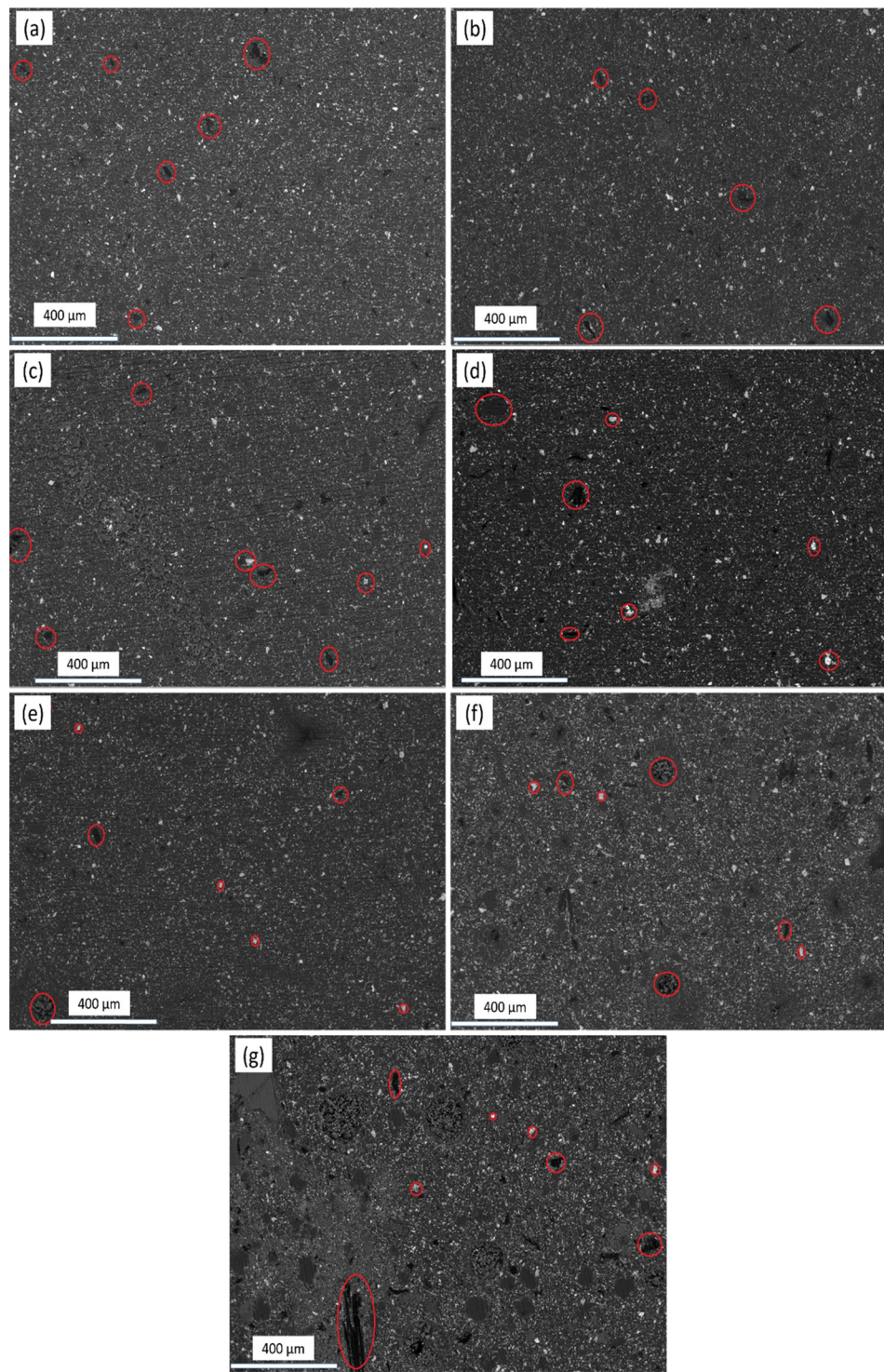


**Fig. 2** SEM micrographs of samples containing: (a) pure  $\text{Al}_2\text{O}_3$ , (b) 10wt% $\text{Al}_2\text{O}_3$ /5wt% $\text{Y}_2\text{O}_3$ , (c) 10wt% $\text{Al}_2\text{O}_3$ /5wt% $\text{Y}_2\text{O}_3$ /0.5wt%GNSs, (d) 10wt% $\text{Al}_2\text{O}_3$ /5wt% $\text{Y}_2\text{O}_3$ /1wt%GNSs, (e) 10wt% $\text{Al}_2\text{O}_3$ /5wt% $\text{Y}_2\text{O}_3$ /1.5wt%GNSs, (f) 10wt% $\text{Al}_2\text{O}_3$ /5wt% $\text{Y}_2\text{O}_3$ /2wt%GNSs, and (g) 10wt% $\text{Al}_2\text{O}_3$ /5wt% $\text{Y}_2\text{O}_3$ /2.5wt%GNSs.

Generally, there is no great difference between the microstructures of all the samples.<sup>22</sup> A good homogenous distribution of all the constituents in the paint matrix was observed. In the microstructure, it appears that the graphene nanosheets have covered the entire area with a small distributions of  $\text{Al}_2\text{O}_3$  and a smaller distributions of  $\text{Y}_2\text{O}_3$  (Fig. 2).

### 3.2. X-ray powder diffraction

The XRD patterns for  $\text{Al}_2\text{O}_3$ ,  $\text{Y}_2\text{O}_3$ , and graphene, and for composite powders of 10wt% $\text{Al}_2\text{O}_3$ /5wt% $\text{Y}_2\text{O}_3$ /0.5wt%GNSs and 10wt% $\text{Al}_2\text{O}_3$ -5wt% $\text{Y}_2\text{O}_3$ /2.5wt%GNSs nanocomposite powder are shown in Fig. 3 and 4, respectively. The presence of sharp mean peaks for  $\text{Al}_2\text{O}_3$  and  $\text{Y}_2\text{O}_3$  in the two samples of

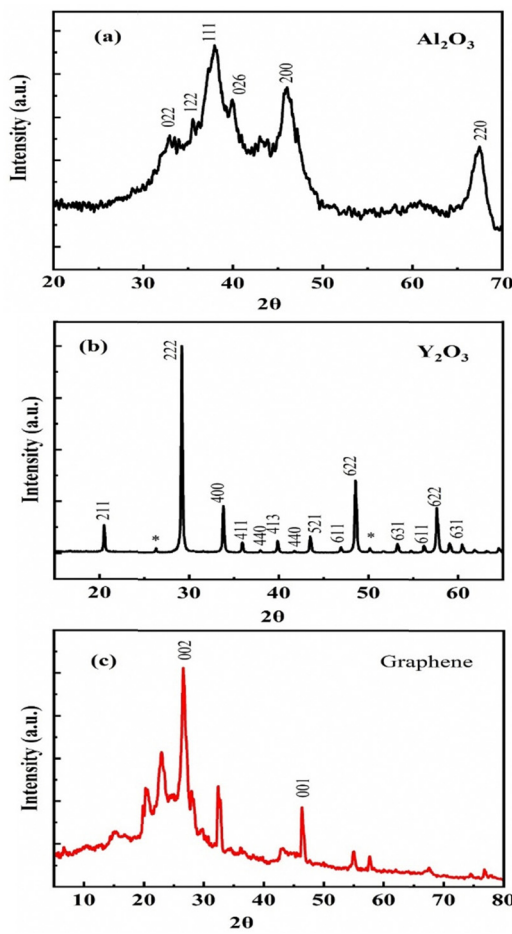


Fig. 3 The XRD test of element powders and mixture powders (a)  $\text{Al}_2\text{O}_3$  powder, (b)  $\text{Y}_2\text{O}_3$  powder, (c) graphene powder.

0.5wt% and 2.5wt% doped-graphene can be observed. However for the samples containing a low GNS ratio, carbon core peaks were not detected. Moreover, the undesirable  $\text{Al}_4\text{C}_3$  carbide phase did not appear. But for the samples containing a low GNS ratio (5), the carbon peaks did not exist because the XRD device cannot detect ratios lower than 2%.<sup>27</sup> The Raman spectrum of graphene is presented in the upper panel of Fig. 4(a) to confirm the structure of graphene.

### 3.3. Thermal analysis (TGA/DSC)

Thermal analysis (TGA/DSC) is a standard technique used to analyze materials with temperature. TGA involves estimation of the weight loss during an applied heating process. But differential scanning calorimetry (DSC) can show whether the sample absorbs or emits energy during heating. In this research, experiments were done on paint samples containing 0.5wt% and 2.5wt% GNSs only.

**3.3.1. Thermogravimetric analysis (TGA) for a 0.5wt% graphene nanosheet sample.** Fig. 5 shows the curves for decomposition of fire-retardant coating during two temperature stages from 55 to 201 °C and from 201 to 400 °C. The first stage at 55–201 °C, due to the dehydration and volatilization of any moisture from internal gases, corresponds to a small mass which is

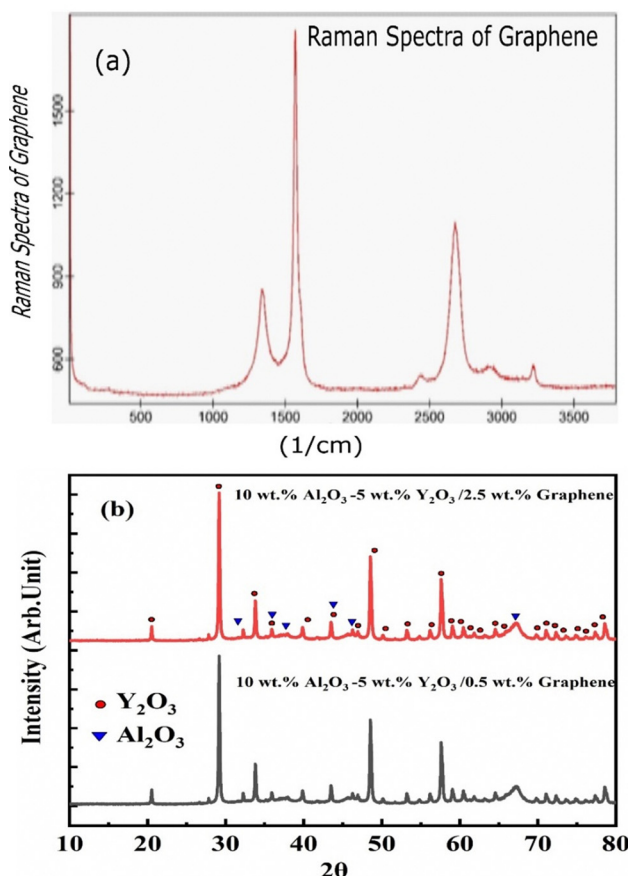


Fig. 4 (a) the Raman spectra of graphene powder, and (b) 10wt% $\text{Al}_2\text{O}_3$ /5wt% $\text{Y}_2\text{O}_3$ /2.5wt%GNSs and 10wt% $\text{Al}_2\text{O}_3$ /5wt% $\text{Y}_2\text{O}_3$ /0.5wt%GNSs nanocomposite powders.

equivalent to a small weight loss (less than 12% by weight). The second stage ranging from 210 °C to 400 °C results from the removal of the basecoat and yttrium oxide composition,<sup>25</sup> consistent with a strong (TGA) peak and large weight loss (>55wt%), which forms the coke bed. The primer breaks down to release a non-combustible gas, which leads to the formation of bulging char.

**3.3.2. Thermogravimetric analysis (TGA) of a 2.5wt% graphene nanosheet sample.** A specific heat curve for the fire-resistant layers is shown in Fig. 5, and the curves for fire-resistant coating basically show decomposition in two stages at temperatures ranging from 65 to 210 °C and from 210 to 400 °C. The first stage at 65–210 °C is caused by the dehydration and volatilization of a small amount of decomposed water and gases, which is equivalent to a small weight loss of graphene (less than 25% by weight). The second stage from 210 to 400 °C,<sup>28,29</sup> results from the removal of the base layer and the combination of aluminum oxide with a mixture of yttrium acetate, consistent with a strong (TGA) peak and large mass loss (>75wt%), which forms the charred layer. The primer breaks down to release a non-combustible gas, creating a layer of smoldering black char. TGA for the sample containing 2.5wt% GNSs provides an indication for determining the quantitative composition of graphene and

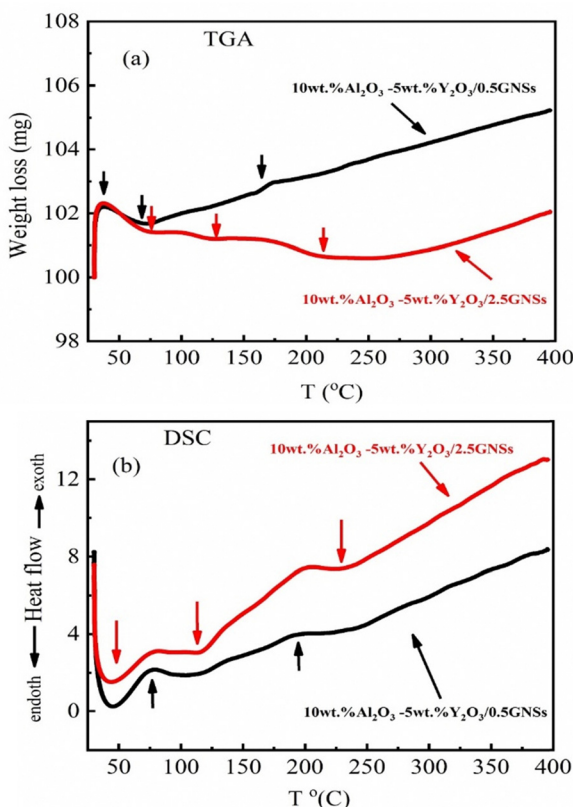


Fig. 5 Thermal analysis (TGA/DSC) of samples with 0.5wt% and 2.5wt% of graphene.

the presence of impurities such as graphite and graphene oxide particles.

#### 3.4. XPS study of the samples

**3.4.1. Comparison between oxygen and aluminum atoms using XPS experiments.** The curves for two oxygen atoms with aluminum atoms are shown in Fig. 6. It can be seen that the number of atoms present in aluminum oxide is equivalent to the atoms present in oxygen,<sup>23</sup> from which the strength and hardness of the mixture sample can be increased at a total energy of 75 eV at the equivalent of 1200 cps, and thus we note the extent of the equivalence of the two oxygen atoms with an atom of aluminum in the mixture.<sup>24</sup>

**3.4.2. Comparison of oxygen and aluminum atoms using XPS experiments.** The curves for two oxygen atoms with aluminum atoms are shown in Fig. 6. The number of atoms present in aluminum oxide is equivalent to the number of atoms present in oxygen, from which the strength and hardness of the mixture can increase the sample with total energies of 158 eV and 158 eV at the equivalent of 4200 cps and 4600 cps. Thus, the clarity of the aluminum strip improved significantly due to the high proportion of oxygen atoms.

**3.4.3. Comparison between Al<sub>2</sub>O<sub>3</sub>/Y<sub>2</sub>O<sub>3</sub>/GNSs nanocomposites using XPS experiments.** The curves used in the test were displayed between aluminum oxide atoms and yttrium oxide and graphene atoms used in the mixture at 500 eV and between 9000

cps. The sector shows an interconnectedness between the atoms in the mixture, which shows the extent of the integration of the mixture and some of them in one sector are shown in Fig. 6 and Table 2.

#### 3.5. Fire combustion test and the mixture's ability to resist fire

As a requirement for building and furniture safety, the safety and reliability of wooden doors are the main aspects determining their effectiveness during a fire.<sup>27</sup> In this research, there are only experimental prototypes, and the lowest equilibrium temperature was selected for the fire endurance test and temperature rise tests to compare the fire resistance rating and heat transfer rate by visual observation/examination. Fire endurance testing was established to determine the ability of fire-rated wooden material prototypes to survive a specified fire condition for a certain period of time without a major safety defect or leak. In this research, an experiment testing 8 mm thick pieces of wood serves as a prototype for a commercial fireproof door. The results of the fire tolerance and temperature rise of the prototypes after a fire of a certain duration were recorded. Several models achieved fire resistance ratings for certain durations without safety failures or significant fire leaks occurring.<sup>28</sup>

Fig. 7(c) shows that samples of wood coated with paints of mixed powders had the highest rate of fire resistance compared to the samples of pure wood shown in Fig. 7(a), and the samples of wood coated with paint shown in Fig. 7(b). The result for the pure wood sample in Fig. 7(a) shows a level of heat resistance of 35 s, while the result for the sample of wood coated with paint in Fig. 7(b) shows an increase in the level of heat resistance of 90 s. In addition, the results for the samples of wood coated with a paint of mixed powders in Fig. 7(c) show an increasing level of heat resistance due to the increasing influence of GNSs wt% for 10wt%Al<sub>2</sub>O<sub>3</sub>/5wt%Y<sub>2</sub>O<sub>3</sub>/x wt%GNSs (x: 0, 0.5, 1.0, 1.5, 2.0, 2.5). The results in Fig. 7(c) show the increased fire resistance of these samples compared with the pure wood sample and samples of wood coated with paint, shown in Fig. 7(a) and (b).

The highest rate of fire resistance was found for wood treated with paint with 10wt%Al<sub>2</sub>O<sub>3</sub>/5wt%Y<sub>2</sub>O<sub>3</sub>/2.5wt%GNSs compared to all the other samples, while the sample of wood treated with paint with 10wt%Al<sub>2</sub>O<sub>3</sub> shows an unexpected level of heat resistance, containing aluminum oxide alone, which showed special fire resistance results.<sup>29</sup> It contains less additives than the rest of the samples, despite the presence of quantities of yttrium oxide and aluminum oxide as shown in Fig. 8, while a sample of wood treated with paint with 10wt%Al<sub>2</sub>O<sub>3</sub>/5wt%Y<sub>2</sub>O<sub>3</sub>/0.5wt%GNSs has a natural fire resistance rate due to the quantities at the beginning plus the addition of 0.5 g of graphene to give high stability and natural resistance. Moreover, the wood treated with paint with 10wt%Al<sub>2</sub>O<sub>3</sub>/5wt%Y<sub>2</sub>O<sub>3</sub>/1wt%GNSs shows that the addition of 1 g of graphene led to a higher resistance to fire at a temperature of 110 °C, while the sample of wood treated with paint with 10wt%Al<sub>2</sub>O<sub>3</sub>/5wt%Y<sub>2</sub>O<sub>3</sub>/1.5wt%GNSs with an increase in the proportion of graphene to 1.5 g led to higher resistance and more smoke than the other samples, and similarly with an increase in graphene to 2 g, as shown in Fig. 7(c) and 8.



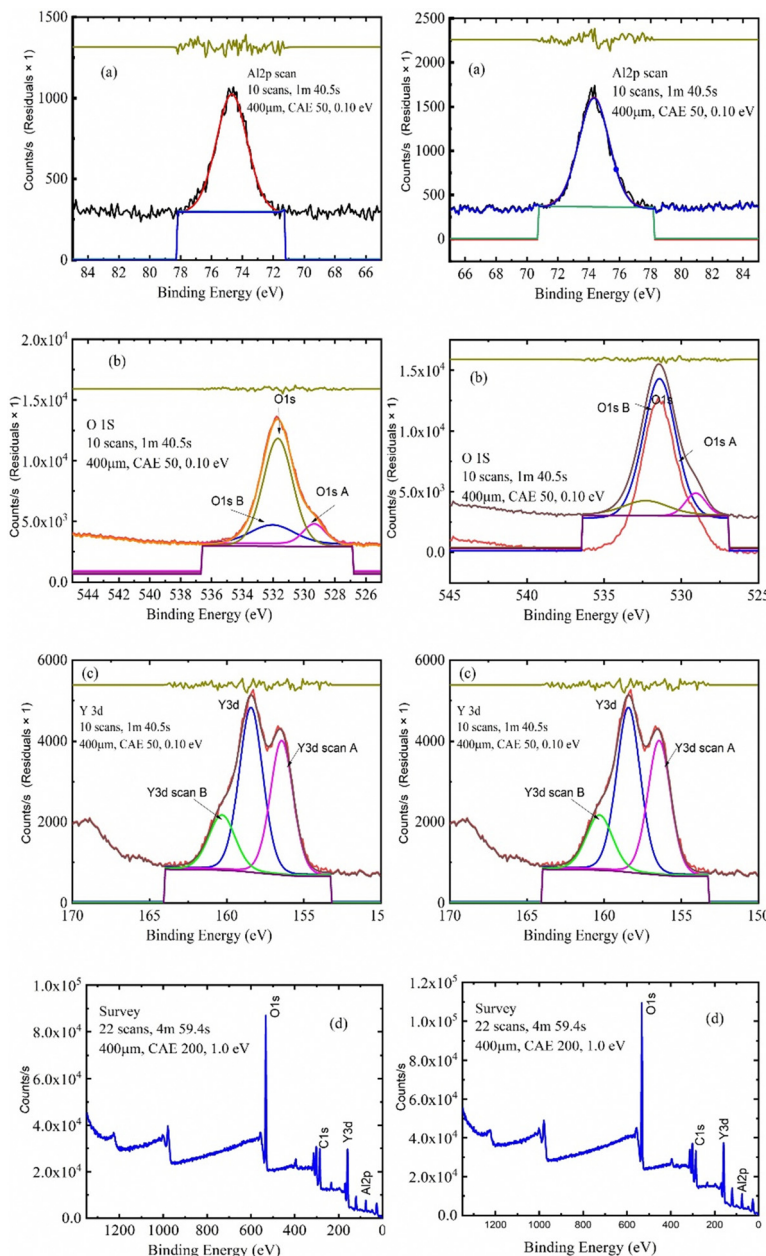


**Fig. 6** A comparison of oxygen and aluminum atoms at 75 eV at the equivalent of 1200 cps. A comparison of oxygen atom and aluminum atoms at 158 eV and 158 eV at the equivalent of 4200 cps and 4600 cps. A comparison of  $\text{Al}_2\text{O}_3/\text{Y}_2\text{O}_3/\text{GNSs}$  nanocomposite atoms at 158 eV and 158 eV at the equivalent of 4200 cps and 4600 cps.

In addition, this led to a greater resistance to fire due to the consistency of the mixture and the lack of carbonization of graphene with the intensity of heat, compared to the sample of wood treated with paint with 10wt% $\text{Al}_2\text{O}_3$ /5wt% $\text{Y}_2\text{O}_3$ /2.5wt%GNSs in Fig. 7(c). This sample in Fig. 7(c) shows the largest percentage of fire resistance compared with other samples from previous research, such as,<sup>30–32</sup> whose temperature was 185 °C with a fire resistance value of 518 s.<sup>30</sup> In addition, the percentage of additives was non-existent, which led to a fire igniting in the sample as soon as the experiment began. This was due to the lack of additives in the plywood, which led very

**Table 2** The results of a comparison of  $\text{Al}_2\text{O}_3/\text{Y}_2\text{O}_3/\text{GNSs}$  nanocomposites

Name	Peak BE	FWHM (eV)	Area (P) cps (eV)	Atomic (%)	Q
O1s	532.3	4.13	374 778.6	65.55	1
$\text{Y}_3\text{d}$	159.03	5.1	152 505.4	10.72	1
C1s	285.71	4.01	78 284.41	0	0
Al <sub>2</sub> p	75.4	3.95	31 447.92	23.73	1
Name	Peak BE	FWHM (eV)	Area (P) cps (eV)	Atomic (%)	Q
O1s	532.37	4.02	282 021	68.52	1
$\text{Y}_3\text{d}$	159.31	5.16	122 203.7	11.93	1
C1s	285.76	3.86	74 831.32	0	0
Al <sub>2</sub> p	75.74	3.55	18 641.52	19.54	1



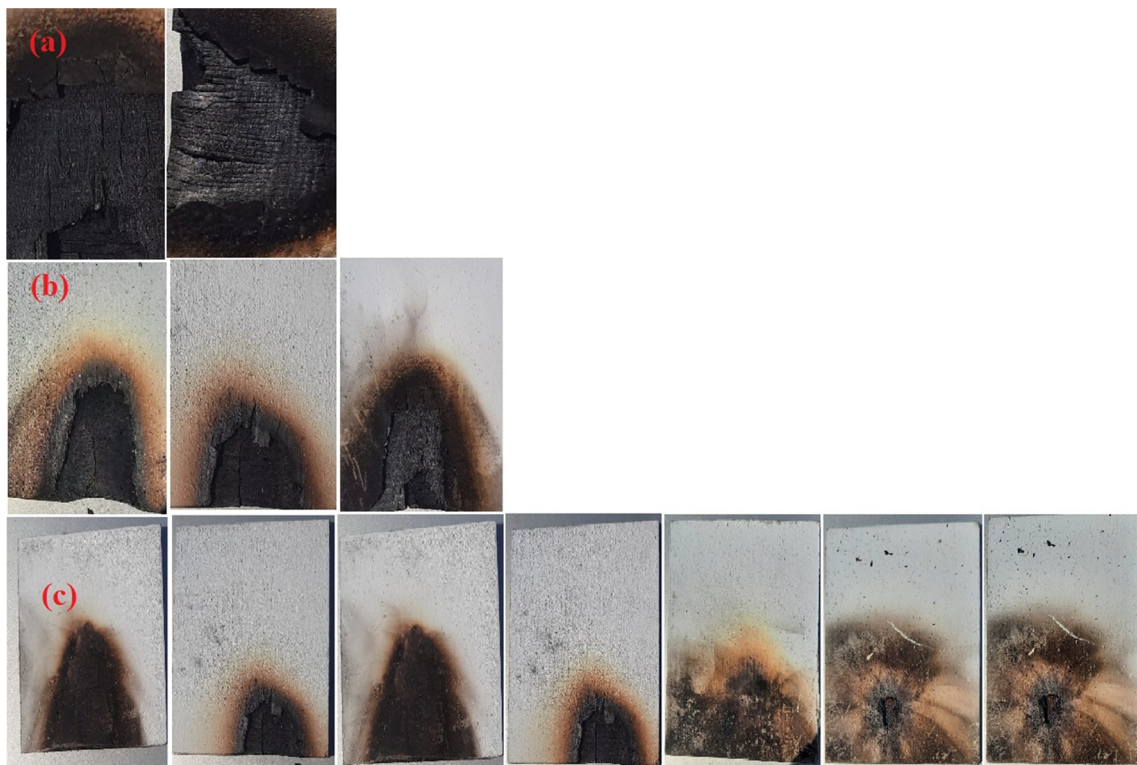


Fig. 7 Wood samples after the fire resistance test: (a) pure wood samples; (b) wood samples treated with paint; (c) wood samples coated with paints of mixed powders: 10wt%Al<sub>2</sub>O<sub>3</sub> and 10wt%Al<sub>2</sub>O<sub>3</sub>/5wt%Y<sub>2</sub>O<sub>3</sub>/xwt%GNSs (x: 0, 0.5, 1.0, 1.5, 2.0, 2.5), respectively.

quickly to charring of the plywood, not reaching 35 s,<sup>31</sup> which is a very weak period compared to the rest of the experiments, while the research sample, which was a sample with paint with 10wt%Al<sub>2</sub>O<sub>3</sub>/5wt%Y<sub>2</sub>O<sub>3</sub>/2.5wt%GNSs, which contains 2.5 g of

graphene, had a fire resistance of 887 s and a temperature of about 190 °C. Thus, the results confirm that the sample with paint with 10wt%Al<sub>2</sub>O<sub>3</sub>/5wt%Y<sub>2</sub>O<sub>3</sub>/2.5wt%GNSs is the most fire resistant with a greater fire resistance time.

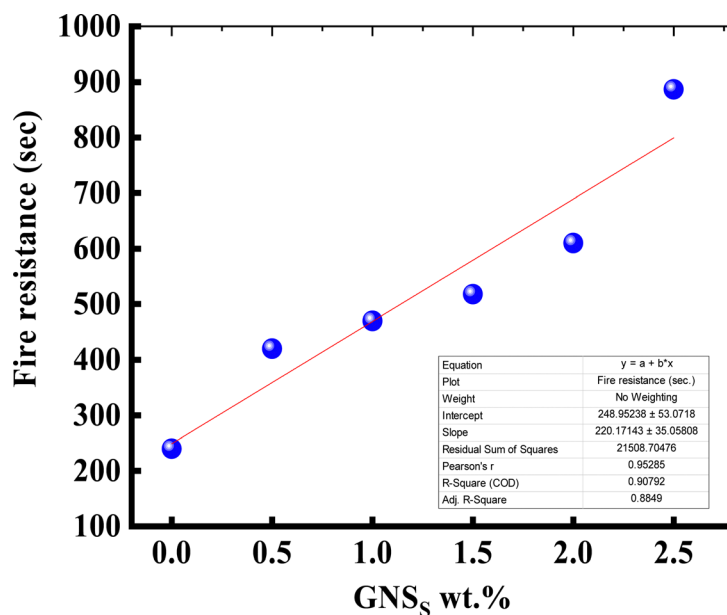


Fig. 8 The effect of GNS content on the fire resistance of wood samples coated with paint with 10wt%Al<sub>2</sub>O<sub>3</sub> and 10wt%Al<sub>2</sub>O<sub>3</sub>/5wt%Y<sub>2</sub>O<sub>3</sub>/xwt%GNSs (x: 0, 0.5, 1.0, 1.5, 2.0, 2.5) mixed powders.



## 4. Conclusions

A surface coating treatment consisting of wood paint with different percentages of mixtures formed of 10wt% $\text{Al}_2\text{O}_3$ /5wt% $\text{Y}_2\text{O}_3$ /xwt%GNSs ( $x$ : 0, 0.5, 1.0, 1.5, 2.0, 2.5) has been used to provide different percentages of fire-retardant coatings on the surface area to check fire resistance and thermal stability. The surface area of graphene was 135, 212, and 244  $\text{m g}^{-1}$ , respectively. The experimental results indicated that the addition of graphene to yttrium oxide in the presence of a constant amount of the base, aluminum oxide, can improve the thermal stability and antioxidant properties of the inorganic expansion layer.<sup>32</sup> The final temperature was 200 °C. The 2.5wt% graphene-laminated structure can form a dense structure with a high expansion factor, and can effectively isolate heat transfer. The fire resistance test showed that the amount of graphene added to yttrium oxide with aluminum oxide led to good cohesion of the mixture and sufficient resistance to fire. The smoke resistance of the sample is minimal and non-existent. The results demonstrated that low-cost and easily fabricated  $\text{Al}_2\text{O}_3/\text{Y}_2\text{O}_3/\text{GNSs}$  nanocomposite powders enhanced the properties of the wood-paint to make it a good candidate in fire resistance applications.

## Data availability

The data that support the findings of this study are available from the corresponding author upon reasonable request.

## Ethical approval

No ethical approval was granted to conduct the experiments involved within the manuscript.

## Conflicts of interest

The authors declare that they have no known competing financial interests or personal relationships that could have appeared to influence the work reported in this paper.

## Acknowledgements

The authors would like to thank Dr Ahmed Mukhtar for his discussion of the XPS data.

## References

- 1 A.-L. Davesne, *et al.*, Thin coatings for fire protection: An overview of the existing strategies, with an emphasis on layer-by-layer surface treatments and promising new solutions, *Prog. Org. Coat.*, 2021, **154**, 106217.
- 2 M. Yew, *et al.*, Fire propagation performance of intumescent fire protective coatings using eggshells as a novel biofiller, *Scientif. World J.*, 2014, **4207**, 805094.
- 3 W. Puspitasari, *et al.*, The study of adhesion between steel substrate, primer, and char of intumescent fire retardant coating, *Prog. Org. Coat.*, 2019, **127**, 181–193.
- 4 G. Malucelli and M. Barbalini, UV-curable acrylic coatings containing biomacromolecules: A new fire retardant strategy for ethylene-vinyl acetate copolymers, *Prog. Org. Coat.*, 2019, **127**, 330–337.
- 5 Z. Qin, *et al.*, Prediction of BeiDou satellite orbit Maneuvers to improve the reliability of real-time navigation products, *Remote Sens.*, 2021, **13**(4), 629.
- 6 X. Wang, *et al.*, Influence of  $\text{Cr}_2\text{O}_3$  particles on corrosion, mechanical and thermal control properties of green PEO coatings on Mg alloy, *Ceram. Int.*, 2022, **48**(3), 3615–3627.
- 7 Z. Miao, *et al.*, Accident Consequence Simulation Analysis of Pool Fire in Fire Dike, *Procedia Eng.*, 2014, **84**, 565–577.
- 8 N. Chulikavit, *et al.*, Thermal degradation and flame spread characteristics of epoxy polymer composites incorporating mycelium, *Sci. Rep.*, 2023, **13**(1), 17812.
- 9 S. Dong, *et al.*, Polydopamine enwrapped titanium dioxide-assisted dispersion of graphene to strength fire resistance of intumescent waterborne epoxy coating, *Prog. Org. Coat.*, 2021, **157**, 106291.
- 10 T. Eremina, D. Korolchenko and D. Minaylov, Experimental Evaluation of Fire Resistance Limits for Steel Constructions with Fire-Retardant Coatings at Various Fire Conditions, *Sustainability*, 2022, **14**(4), 1962.
- 11 O. Y. Wen, *et al.*, Fire-resistant and flame-retardant surface finishing of polymers and textiles: A state-of-the-art review, *Prog. Org. Coat.*, 2023, **175**, 107330.
- 12 U. A. Rosemary, *et al.*, Studies on the Effectiveness of Flame Retardant Paint Treatment of Timbers, *Middle-East J. Scientif. Res.*, 2014, **21**(9), 1652–1654.
- 13 W. Yang, *et al.*, Nanoparticles of polydopamine for improving mechanical and flame-retardant properties of an epoxy resin, *Compos., Part B*, 2020, **186**, 107828.
- 14 M. C. Yew, *et al.*, Fire Propagation Performance of Intumescent Fire Protective Coatings Using Eggshells as a Novel Biofiller, *Scientif. World J.*, 2014, **2014**, 805094.
- 15 L. D. Mathews, *et al.*, Recent progress and multifunctional applications of fire-retardant epoxy resins, *Mater. Today Commun.*, 2022, **33**, 104702.
- 16 S. Agnihotri, *et al.*, Flame-retardant textile structural composites for construction application: a review, *J. Mater. Sci.*, 2024, **59**, 1788–1818.
- 17 E. Shim, *2 - Coating and laminating processes and techniques for textiles*, in *Smart Textile Coatings and Laminates*, ed. W. C. Smith, 2010, Woodhead Publishing. 10–41.
- 18 S. Chen, *et al.*, Facile fabrication of superhydrophobic, flame-retardant and conductive polyurethane sponge via dip-coating, *Mater. Lett.*, 2021, **287**, 129307.
- 19 L. Calabrese, *et al.*, Thermal characterization of intumescent fire retardant paints, *J. Phys.: Conf. Ser.*, 2014, **547**, 012005.
- 20 R. Olawoyin, Nanotechnology: The future of fire safety, *Safety Sci.*, 2018, **110**, 214–221.



21 H. Yang, *et al.*, Surface-coating engineering for flame retardant flexible polyurethane foams: A critical review, *Comp., Part B*, 2019, **176**, 107185.

22 W. Yang, *et al.*, Graphene oxide-based noble-metal nanoparticles composites for environmental application, *Composit. Commun.*, 2021, **24**, 100645.

23 M. S. Chavali and M. P. Nikolova, Metal oxide nanoparticles and their applications in nanotechnology, *SN Appl. Sci.*, 2019, **1**(6), 607.

24 A. I. Ali, *et al.*, Preparation, structural and dielectric properties of nanocomposite  $\text{Al}_2\text{O}_3/\text{BaTiO}_3$  for multilayer ceramic capacitors applications, *J. Mater. Res. Technol.*, 2022, **18**, 2083–2092.

25 A. I. Ali, S. A. Salim and E. A. Kamoun, Novel glass materials-based (PVA/PVP/ $\text{Al}_2\text{O}_3/\text{SiO}_2$ ) hybrid composite hydrogel membranes for industrial applications: synthesis, characterization, and physical properties, *J. Mater. Sci.: Mater. Electron.*, 2022, **33**(13), 10572–10584.

26 A. E.-R. T. AboZied, *et al.*, Structure, magnetic and magnetocaloric properties of nano crystalline perovskite  $\text{La}_{0.8}\text{Ag}_{0.2}\text{MnO}_3$ , *J. Magn. Magn. Mater.*, 2019, **479**, 260–267.

27 H. Abd El-Wahab, *et al.*, Synthesis and characterisation of sulphonamide (Schiff base) ligand and its copper metal complex and their efficiency in polyurethane varnish as flame retardant and antimicrobial surface coating additives, *Prog. Org. Coat.*, 2020, **142**, 105577.

28 A. S. Gandhi and C. G. Levi, Phase selection in precursor-derived yttrium aluminum garnet and related  $\text{Al}_2\text{O}_3\text{--Y}_2\text{O}_3$  compositions, *J. Mater. Res.*, 2005, **20**(4), 1017–1025.

29 C. Ullal, *et al.*, Non-equilibrium phase synthesis in  $\text{Al}_2\text{O}_3\text{--Y}_2\text{O}_3$  by spray pyrolysis of nitrate precursors, *Acta Mater.*, 2001, **49**(14), 2691–2699.

30 R. H. White, Fire resistance of wood members with directly applied protection, *Fire Mater.*, 2009, 971.

31 J.-H. Lee, Y.-S. Sohn and S.-H. Lee, Fire resistance of hybrid fibre-reinforced, ultra-high-strength concrete columns with compressive strength from 120 to 200 MPa, *Mag. Concr. Res.*, 2012, **64**(6), 539–550.

32 T. Lie, Optimum fire resistance of structures, *J. Struct. Div.*, 1972, **98**(1), 215–232.

